JOURNAL OF MAGNETIC RESONANCE **131,** 203–208 (1998)
ARTICLE NO. MN971349

Demonstrating the Spatial Resolution of Field Gradient NMR

T. Feiweier, B. Geil, O. Isfort, and F. Fujara

Fachbereich Physik, Universität Dortmund, D-44221 Dortmund, Germany

Received August 19, 1997; revised November 26, 1997

In recent years, field gradient NMR has become a method of increasing importance in measuring very small dislocations of molecules. Rough estimations indicate that, by utilizing large field gradients, one should be able to detect motions down to the 10-nm scale. However, this limit has not yet been experimentally detected. In this paper, we present a method that allows the direct measurement of the spatial resolution of field gradient NMR. For our experimental setup, utilizing an extremely large static field gradient of about 180 T m^{-1}, we find a lower limit of 7 nm, thus for the first time confirming the expected resolution. Furthermore, we discuss the effect of unwanted vibrations as a limiting factor of the method.

Key Words: **field gradient NMR; dynamical imaging; spatial resolution; oscillation; polymer.**

INTRODUCTION

The analogy between the stimulated echo diffusion experiment in field gradient NMR and scattering experiments was for the first time pointed out by Hertz (*1*) and later taken up by others (see, for instance, (*2–5*)). It raises the question of how these methods compare with each other with respect to the dynamical ranges covered. While the time scales available to the experiments are completely different (10^{-3} to 10^{0} s for NMR, 10^{-12} to 10^{-9} s for neutron scattering), this does not hold for the spatial resolution. Neutron scattering is sensitive to motions with amplitudes in the range from 0.01 to 10 nm. Large spatial dislocations on the micrometer scale have been extensively measured with NMR methods (*6, 7*), but no experiment so far proved the theoretical estimation (*8, 9*) of a lower limit better than 10 nm.

In this paper, we describe an experiment that directly demonstrates the spatial resolution of field gradient NMR. The basic principle is rather simple; the whole sample is mechanically moved, i.e., oscillated sinusoidally with well-defined frequency and amplitude. As a translatory motion in the inhomogenous magnetic field, these oscillations show up in the stimulated echo decay. The smallest amplitude that still affects the attentuation curve then gives us the resolution limit we are looking for. We should note that one must be careful with the meaning of ''spatial resolution.'' It does not mean, as in common imaging experiments, the smallest fraction of the sample we can selectively look at. Rather, we examine the sample as a whole and use the dynamics of a moving spin species to explore structure and dynamics on a microscopic scale. In this case, one would better speak of a ''dynamical spatial resolution,'' thus also referring to the terminology of ''dynamical imaging'' sometimes applied for this technique.

By quantitatively evaluating the effect oscillations have on field gradient NMR, we also gain insight into the influence of unwanted vibrations by various sources (e.g., building vibrations). These turn out to impose limits on the experiment. Problems of this kind have been reported in the past (*8, 10*).

THEORY

First of all, we must analyze the effect of a coherent oscillation of all nuclear spins on the stimulated echo decay curve. Figure 1 shows the stimulated echo pulse sequence. Since we use a static field gradient (SFG NMR), as shown in Fig. 2, no gradient pulses are necessary (*11*). The amplitude of the stimulated echo can be written as a one-particle correlation function multiplied by two factors that take into account the spin–spin (T_2) and spin–lattice relaxation (T_1) (*12, 13*).

Let us take the normalized echo amplitude S as a starting point,

$$S(\boldsymbol{Q}, t) = e^{-2\tau/T_2} \cdot e^{-t/T_1} \cdot \langle e^{-i\boldsymbol{Q}\boldsymbol{r}(0)} e^{i\boldsymbol{Q}\boldsymbol{r}(t)} \rangle, \qquad [1]$$

where the dephasing time τ and mixing time t are defined in Fig. 1, the generalized scattering vector $\boldsymbol{Q}$ is given by $\boldsymbol{Q} = \gamma \boldsymbol{g} \tau$ (gyromagnetic ratio γ, magnetic field gradient $\boldsymbol{g}$), and $\boldsymbol{r}(0)$ and $\boldsymbol{r}(t)$ denote the positions of a nuclear spin at times 0 and t, respectively. As in scattering experiments, $\boldsymbol{Q}^{-1}$ indicates the spatial displacements the experiment looks at. The term inside the angle brackets is to be evaluated as an ensemble average over all spins, taking into account the probability of a spin moving from $\boldsymbol{r}(0)$ to $\boldsymbol{r}(t)$ within the time t. As an example, consider a free Fickian diffusion with diffusion coefficient D. In this case the probability function,

1090-7807/98 $25.00

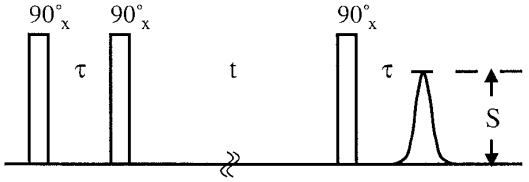

FIG. 1. Stimulated echo pulse sequence, $(\pi/2)_x-\tau-(\pi/2)_x-t-(\pi/2)_x-\tau-$echo, consisting of dephasing time τ, mixing time t, and rephasing time τ. With field gradient NMR, the attenuation of the echo amplitude indicates translatory motion within the mixing time. The condition $\tau < T_2 \ll t < T_1$ must be fulfilled.

often called the propagator, takes the form of a Gaussian giving rise to the well-known equation

$$S_D(\boldsymbol{Q}, t) = e^{-2\tau/T_2} \cdot e^{-t/T_1} \cdot e^{-Q^2Dt}. \qquad [2]$$

Now we must examine an oscillatory motion of the spins with angular frequency Ω, amplitude $\boldsymbol{R}$, and phase ϕ at the beginning of the pulse sequence, which is parametrized by

$$\boldsymbol{r}(t) = \boldsymbol{r}_0(t) + \boldsymbol{R}\sin(\Omega t + \phi). \qquad [3]$$

By adding a time-dependent offset $\boldsymbol{r}_0(t)$, we still take into account the superposition of a diffusive process. Taking together Eqs. [1] and [3], and noticing the fact that the oscillation is not of statistical nature, we get for the stimulated echo decay

$$S(\boldsymbol{Q}, t) = e^{-2\tau/T_2} \cdot e^{-t/T_1} \cdot \langle e^{-i\boldsymbol{Q}\boldsymbol{r}_0(0)} e^{i\boldsymbol{Q}\boldsymbol{r}_0(t)} \rangle \cdot e^{i\boldsymbol{Q}\boldsymbol{R}[\sin(\Omega t+\phi)-\sin(\phi)]}, \qquad [4]$$

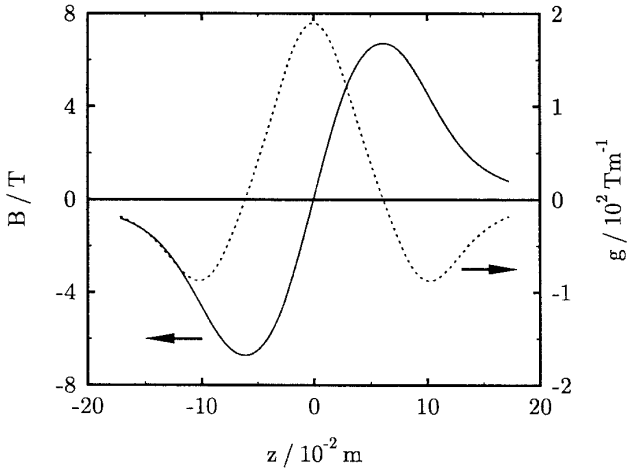

FIG. 2. Plot of the magnetic field profile (—) and gradient (---) along the room-temperature bore.

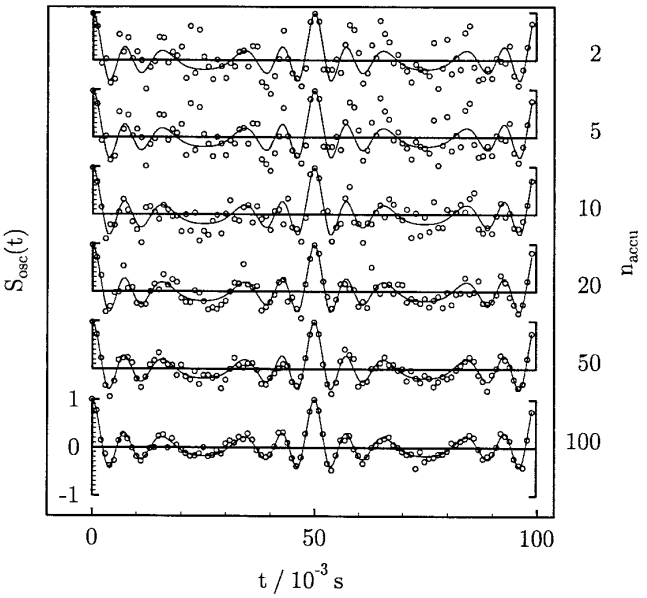

FIG. 3. Simulation of an oscillation experiment (frequency: 50 Hz) with n_{accu} numbers of accumulations. Solid line: theory curve ($n_{accu} \to \infty$). For at least 100 accumulations, theory and simulations agree well.

where the first two terms account for relaxation, the third accounts for diffusion, and the last one accounts for the oscillatory motion. All experiments were performed once with and once without an oscillating sample, so that, by dividing Eq. [4] through Eq. [1], we can proceed to the relaxation- and diffusion-normalized correlation function

$$S'_{osc}(\boldsymbol{Q}, t) = e^{i\boldsymbol{Q}\boldsymbol{R}(\sin(\Omega t+\phi)-\sin(\phi))}. \qquad [5]$$

Due to the fact that we must accumulate the NMR signal to get an appropriate signal-to-noise ratio and assuming no phase correlation between the oscillation and the repetition frequency of the experiment, we finally must sum over a number of phases ϕ. Having a sufficient number of accumulations, this can be approximated by the integral

$$S_{osc}(\boldsymbol{Q}, t) = \int_0^{2\pi} e^{i\boldsymbol{Q}\boldsymbol{R}(\sin(\Omega t+\phi)-\sin(\phi))} d\phi. \qquad [6]$$

In order to estimate the number of accumulations necessary to justify this approximation, we simulated the experiment. Figure 3 proves that we have to accumulate at least 100 times to get a sufficient agreement. This is the minimum number used in the experiments.

Equation [6] describes the theoretical curve used to analyze and fit our data. We will refer to it as the phase averaged oscillation correlation function. Recognize that it depends only on two parameters, namely the oscillation frequency Ω and the product of scattering vector $\boldsymbol{Q}$ and oscillation ampli-

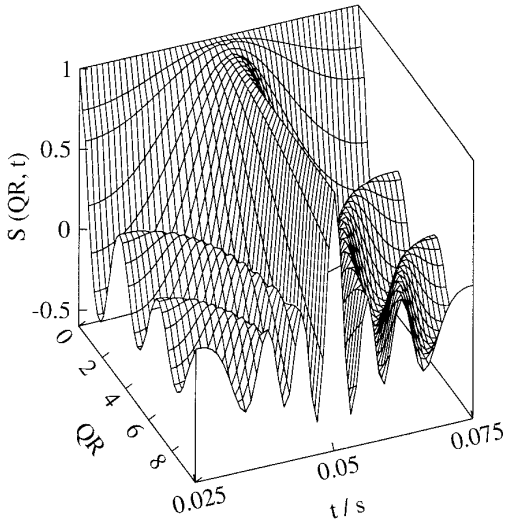

FIG. 4. Theoretically predicted effect of a 20-Hz oscillation on the stimulated echo decay, calculated by Eq. [6] as a function of $\boldsymbol{QR}$ and t. To point out the details, we omitted the time interval from 0 to 0.025 s. The function is periodic in t with a period of 1/20 s.

tude $\boldsymbol{R}$. Figure 4 shows the shape of Eq. [6] as a function of t and $\boldsymbol{QR}$. All experiments shown below measure decay curves with variable t at constant $\boldsymbol{QR}$.

It is fascinating to see how far the analogy between field gradient NMR and scattering experiments reaches. In a recent work Jex *et al.* (*14*) show that a similar formalism holds for Bragg scattering of synchroton radiation by an oscillating quartz crystal.

EXPERIMENTAL SETUP

All measurements were performed with a homebuilt SFG spectrometer. Special attention should be given to the cryomagnet used (Oxford Instruments, Oxford, UK). Utilizing an ''anti-Helmholtz''-like arrangement of coils, field gradients up to 200 T m^{-1} are available (for further details, see (*8*, *15*)). As $\boldsymbol{Q}$ is proportional to the gradient, large gradients are necessary to achieve a high spatial resolution. Special care has been taken to mechanically decouple the magnet system from the environment. A damping setup turns out to be crucial to avoid the influence of vibrations, e.g., of the whole building, since every motion of the sample relative to the magnetic field shows up in the experiment.

The probe head used to oscillate the sample was especially designed for this purpose. It is based on a piezoelectric transposer, available commercially (PI GmbH & Co, Waldbronn, Germany). This transposer, placed outside the magnet, elongates up to 8 μm when a voltage of 120 V is applied. In our experiments, we applied sinusoidal voltages with frequencies of 20 and 40 Hz and amplitudes from about 0.2 to 7 V. The induced mechanical oscillations of the transposer are directly transfered by a stiff tube to a small Teflon block approximately 28 × 16 × 58 mm in size. The radiofrequency transmission line is placed inside the tube. Within the Teflon block, the whole resonant circuit consisting of a tuning capacitor (ceramics type) in series, a parallel matching capacitor (mica type), and a coil carrying the sample is tightly fitted. By doing so, a direct transfer of the oscillations to the sample is achieved. We note that a quantitative estimation of the oscillation amplitude based on the voltage applied to the piezo is not possible due to unavoidable mechanical losses at the junctions. Figure 5 shows the setup scheme.

In the choice of the sample material, we were guided by two aspects. First of all, the diffusion coefficient should be small such that the diffusive motion does not mask the oscillations. At the same time, a long T_2 value is necessary. By limiting the dephasing time τ which is proportional to $\boldsymbol{Q}$, T_2 plays an important role in the maximum resolution achievable. As a sample that meets both conditions at the same time, PDMS (polydimethylsiloxane) with a molecular weight of 603,000 is chosen (purchased from Polymer Standard Service, Mainz, Germany). For this polymer, we measured a diffusion coefficient of $D = 2.0 \times 10^{-15}$ m^2 s^{-1} at a temperature of 287 K and estimated a spin–spin relaxation time of $T_2 \geq 3 \times 10^{-3}$ s. Thus, this sample is ideally suited for our purpose.

All experiments were performed at a proton resonance frequency of 95 MHz according to a magnetic field of 2.1 T. For this field, regarding Fig. 2, we find two resonance positions with gradients of 57 and 173 T m^{-1}, respectively. These values are consistently obtained by data of the manufacturer, our own hall probe measurements, and diffusion measurements in H_2O as a sample with a well-known diffusion coefficient.

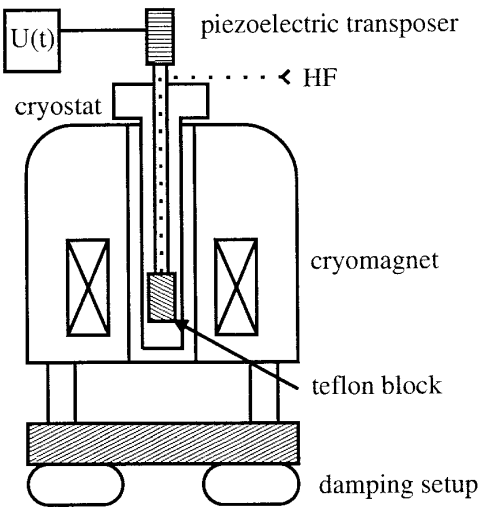

FIG. 5. Experimental setup. For details, refer to the text.

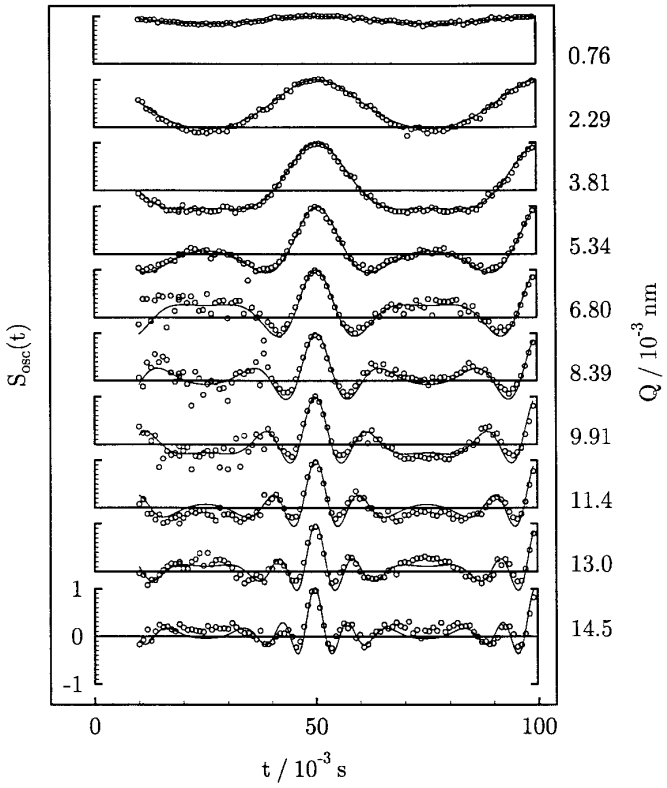

FIG. 6. Series of measurements with oscillating sample (frequency: 20 Hz) in the smaller gradient of 57 T m^{-1}. Different $\boldsymbol{Q}$ values have been realized by adjusting τ. Solid lines represent best fits to Eq. [6]. The oscillation amplitude for all measurements is $\boldsymbol{R} = 535$ nm.

RESULTS

To test our theoretical predictions, we first looked at experiments performed in the field gradient of only 57 T m^{-1}. Figure 6 shows the results of a set of measurements. The only parameter that discerns these measurements is the scattering vector. $\boldsymbol{Q}$ is varied from 0.76×10^{-3} to 14.5×10^{-3} nm^{-1} by choosing different dephasing times τ. As noted earlier, we measured once with and once without oscillations, and all results are shown in normalized form. The data are fitted to Eq. [6] by a least-squares algorithm. We point out the fact that the only free parameter in this procedure is the amplitude $\boldsymbol{R}$ of the oscillation. Comparing experiments with theoretical predictions in Fig. 6, they obviously fit well. The oscillation amplitude that governs the shape of the entire series is 535 ± 10 nm.

As the next step we took a similar series of measurements in the large gradient of 173 T m^{-1}. This time, larger $\boldsymbol{Q}$ values in the range from 5.65×10^{-3} to 47.3×10^{-3} nm^{-1} and a smaller oscillation amplitude are used. The results are shown in Fig. 7. Obviously the data and the fitted oscillation correlation function Eq. [6] (dotted curve) deviate significantly, especially in the regions between the maxima. A better agreement can be achieved if one considers a distribution in $\boldsymbol{QR}$. In Fig. 7 curves assuming a Gaussian distribution are also plotted, and they agree well with the measured data. With this assumption, we get an oscillation amplitude centered at 156 ± 3 nm with a variance of 35 ± 3 nm which again fits the entire series.

We propose two possible mechanisms responsible for a distribution. First, by regarding the magnetic field calculations of the manufacturer, the field gradient turns out to vary somewhat over the slice of the sample selected in the experiment, thus explaining a distribution in $\boldsymbol{Q}$. For the sample arrangement used, this would account for a distribution width of approximately 10% of the center gradient which is only half of the observed value. Another possibility is a distribution of oscillation amplitudes. One would imagine the highly viscous polymer as some kind of shaken gelatin that shows a lower amplitude at the surface of the surrounding glass tube than in the middle of the sample. Most probably the two mechanisms sum up to the observed effect. We also learn from Fig. 7 that whenever an experiment takes place at small values of the product $\boldsymbol{QR}$, no deviations of the data from Eq. [6] are observable. In fact, the mean

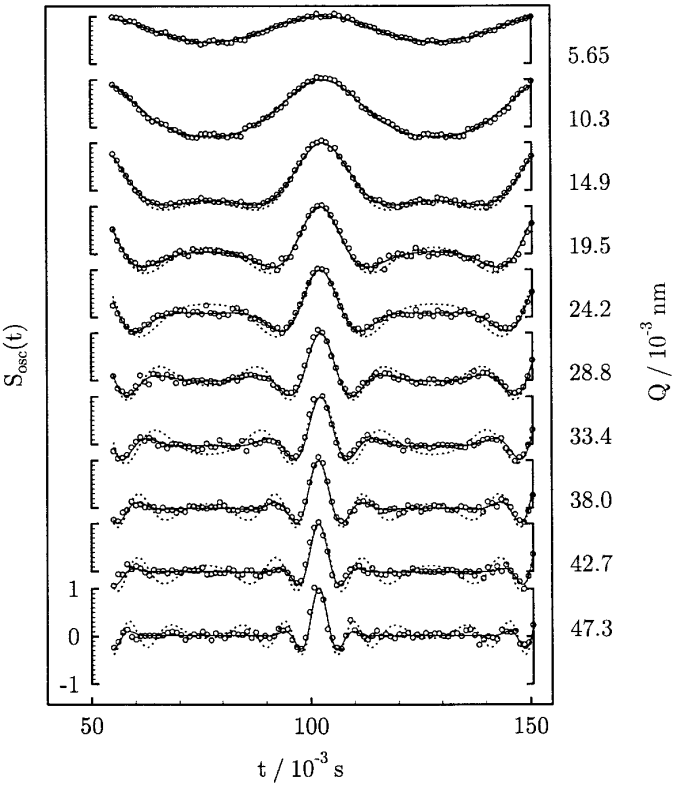

FIG. 7. Analogue to Fig. 6, but in a gradient of 173 T m^{-1}. The axes with $S_{osc} = 0$ have been omitted to exhibit the details. Dotted lines represent best fits to Eq. [6]; for the solid lines a Gaussian distribution in $\boldsymbol{QR}$ has been assumed, leading to a mean amplitude of 156 nm and a variance of 35 nm.

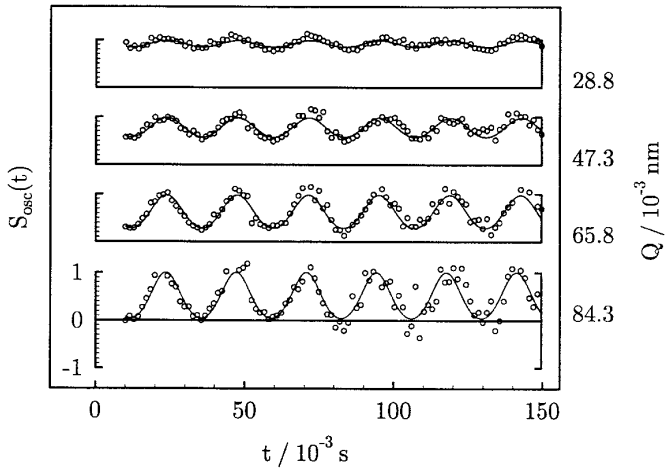

FIG. 8. Series of measurements in the large gradient with an oscillation amplitude of 14 nm. The oscillation frequency here is 40 Hz.

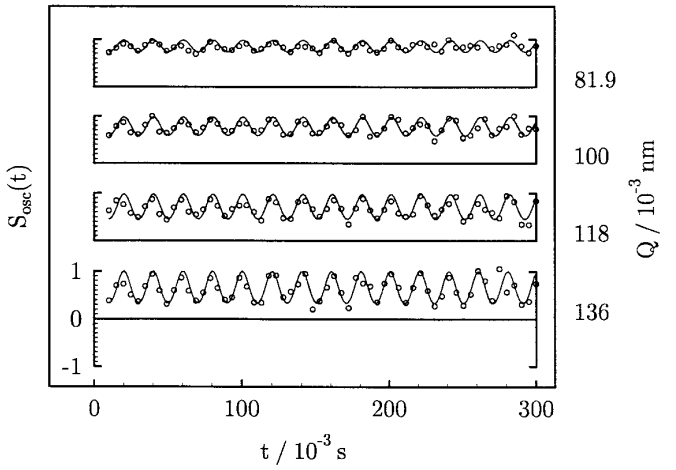

FIG. 10. The effect of a mechanical pump running near the undamped cryomagnet with a vibration frequency of 50 Hz. If the damping setup is enabled, no oscillations show up.

oscillation amplitudes would not be affected by a distribution at all.

We now return to the question of the spatial resolution of field gradient NMR. In Figs. 8 and 9 we present two series of measurements at small oscillation amplitudes that utilize $\boldsymbol{Q}$ values up to 84×10^{-3} nm^{-1}. While the data in Fig. 8 with an amplitude of 14.0 ± 0.5 nm still distinctly display the oscillations, this becomes more spurious in Fig. 9. Here, the diffusive motion starts to dominate. Nevertheless, an amplitude of 6.6 ± 0.4 nm can still be significantly fitted. At the moment, this is the smallest amplitude we have seen. We note that so far this limit is given rather by the imperfect transmission of the piezo oscillations down to the sample. A more sophisticated setup may well permit even smaller amplitudes.

To demonstrate the effect of vibrations in the surrounding of the experimental setup, we ran a mechanical pump (rotary type, vibrating with a frequency of 50 Hz) at a distance of approximately 1 m from the cryomagnet. For this measurement, the damping system was disabled. The data in Fig. 10 clearly indicate the dramatic effect the pump oscillations have on the stimulated echo. They result in an oscillation amplitude of 7.4 ± 0.3 nm of the sample relative to the magnet. If we perform the same experiment with the damping setup enabled, no oscillations show up in the data.

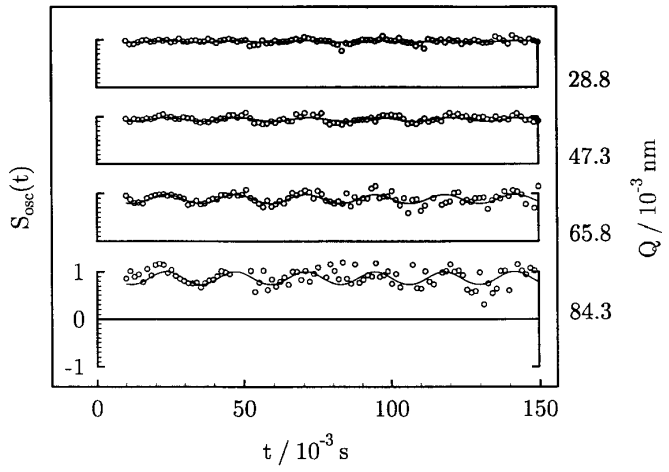

FIG. 9. Resolving the limits: the effect of an oscillation amplitude of 6.6 nm.

CONCLUDING REMARKS

The effect of an oscillatory sample motion on the stimulated echo experiment in field gradient NMR has been discussed in detail. From the theory side, we ended up with an expression for the oscillation correlation function which is directly measurable. Experiments have turned out to be in good agreement with the theoretical predictions. The smallest motion amplitude observable experimentally finally gives us a spatial resolution of field gradient NMR better than 7 nm. However, this holds only for samples that meet the two conditions of slow diffusion and long spin–spin relaxation time. These conditions are ideally exemplified by polymers, thus recommending the method for the study of dynamics in these systems.

We have further shown that vibrations in the surrounding of the magnet affect the stimulated echo experiment if one works with high $\boldsymbol{Q}$ values. In the case of more complicated frequency spectra of the vibrations, they may be less obvious in the attenuation curves. One would expect smaller echo amplitudes or anomalous high scattering in the data due to ''phase noise.'' In the worst case, the decay due to oscillations may be misinterpreted as diffusion, resulting in a too large diffusion coefficient. Our damping setup proves sufficient to suppress these effects.

The main issue of this paper was to demonstrate experimentally the limits of spatial dimensions accessible by field gradient NMR. We have shown that in this respect field gradient NMR closes up with neutron scattering, thus once more illustrating the importance of these two methods as complementary experiments.

ACKNOWLEDGMENT

We gratefully acknowledge the support of our technical staff for setting up the probe head.

REFERENCES

1. H. G. Hertz, Translational motions as studied by nuclear magnetic resonance, *in* ''Molecular Motions in Liquids'' (J. Lascombe, Ed.), pp. 339–341, Reidel, Dodrecht/Holland/Boston (1974).
2. P. T. Callaghan, ''Principles of Nuclear Magnetic Resonance Microscopy,'' Clarendon Press, Oxford (1991).
3. J. Kärger, H. Pfeifer, and W. Heink, *Adv. Magn. Reson.* **12,** 1 (1989).
4. N. F. Fatkullin, *Sov. Phys. JETP* **72,** 563 (1991).
5. R. Kimmich, ''NMR—Tomography, Diffusometry, Relaxometry,'' Springer-Verlag, Berlin/Heidelberg (1997).
6. S. J. Gibbs, *J. Magn. Reson.* **124,** 223 (1997).
7. M. Appel, G. Fleischer, D. Geschke, J. Kärger, and M. Winkler, *J. Magn. Reson. A* **122,** 248 (1996).
8. I. Chang, F. Fujara, B. Geil, G. Hinze, H. Sillescu, and A. Tölle, *J. Non-Cryst. Solids* **172–174,** 674 (1994).
9. P. T. Callaghan and J. Stepisnik, *Phys. Rev. Lett.* **75,** 4532 (1995).
10. N.-K. Bär, J. Kärger, C. Krause, W. Schmitz, and G. Seifert, *J. Magn. Reson. A* **113,** 278 (1995).
11. R. Kimmich, W. Unrath, G. Schnur, and E. Rommel, *J. Magn. Reson.* **91,** 136 (1991).
12. E. L. Hahn, *Phys. Rev.* **50,** 580 (1950).
13. J. E. Tanner and E. O. Stejskal, *J. Chem. Phys.* **49,** 1768 (1968).
14. H. Jex, A. Ludwig, F. J. Hartmann, E. Gerdau, and O. Leupold, *Europhys. Lett.* **40,** 317 (1997).
15. T. Feiweier, O. Isfort, B. Geil, F. Fujara, and H. Weingärtner, *J. Chem. Phys.* **105,** 5737 (1996).